Organic & Biomolecular Chemistry

Cite this: *Org. Biomol. Chem.*, 2011, **9**, 2975

www.rsc.org/obc

PAPER

Disubstituted 2-phenyl-benzopyranopyrimidine derivatives as a new type of highly selective ligands for telomeric G-quadruplex DNA†

Wei-Bin Wu, Shu-Han Chen, Jin-Qiang Hou, Jia-Heng Tan, Tian-Miao Ou, Shi-Liang Huang, Ding Li, Lian-Quan Gu and Zhi-Shu Huang*

Received 23rd October 2010, Accepted 27th January 2011
DOI: 10.1039/c0ob00921k

A series of 2-phenyl-benzopyranopyrimidine (PBPP) derivatives with alkylamino side chains were synthesized and found to be a new type of highly selective ligand to bind with telomeric G-quadruplex DNA, and their biological properties were reported for the first time. Their interactions with telomeric G-quadruplex DNA were studied with FRET melting, surface plasmon resonance, CD spectroscopy, and molecular modeling. Our results showed that the disubstituted PBPP derivatives could strongly bind to and effectively stabilize the telomeric G-quadruplex structure, and had significant selectivity for G-quadruplex over duplex DNA. In comparison, the mono substituted derivatives had much less effect on the G-quadruplex, suggesting that the disubstitution of PBPP is essential for its interaction with the G-quadruplex. Furthermore, telomerase inhibition of the PBPP derivatives and their cellular effects were studied, and compound **11b** was found to be the most promising compound as a telomerase inhibitor and telomeric G-quadruplex binding ligand for further development for cancer treatment.

Introduction

G-quadruplex is a secondary DNA structure formed by guanine-rich sequences, which consists of flat Hoogsteen hydrogen-bonded G-quartets (Fig. 1a).[1,2] Hundreds of thousands of putative quadruplex forming sequences have been identified throughout the genome, such as the telomeric region[3] and some gene promoters,[4,5] opening the intriguing possibility of alternative biological functions. Formation of G-quadruplexes in telomeric DNA results in inhibition of telomerase and extension of telomeres,[6] while G-quadruplexes present in gene promoters are suggested to be involved in the regulation of gene expression.[7,8] Compounds that bind to and stabilize G-quadruplexes have considerable potential to interfere with telomere maintenance[9–11] or regulate oncogene expression.[12,13] Thus, there is a general consensus that G-quadruplex ligands are promising lead compounds for drug discovery and development in cancer therapy. A large number of G-quadruplex interacting ligands have been described.[14] Most of these compounds share common features of functionalized polycyclic aromatic systems such as acridines,[15] anthraquinones,[16] indoloquinolines[17] and porphyrins.[18] More recently, a number of non-polycyclic ligands have been reported including diarylureas,[19] biarylpyrimidines,[20] biaryl polyamides,[21] triarylpyridines,[22] and diarylethynyl amides.[23]

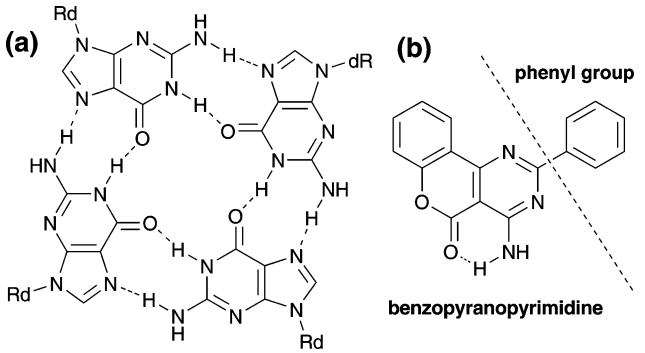

Fig. 1 Structures of G-quartet (a) and the scaffold of PBPPs (b).

Our group has been focused on searching and developing potent and selective G-quadruplex ligands for several years.[17,24,25] Recently, our interest was brought to 2-phenyl-benzopyranopyrimidines (PBPPs, Fig. 1b) because of their unique structural features. To the best of our knowledge, the synthesis of PBPPs has only been reported by a few researchers,[26,27] and their biological applications have remained unexploited. More recently, a couple of PBPPs were found to be high-ranking compounds through virtual screening of fibroblast growth factor receptor 1 kinase inhibitors, but none of these compounds exhibited inhibitory activity in subsequent enzymatic assays.[28] The structure of PBPP comprises a planar moiety of benzopyranopyrimidine, conjugated with a phenyl group by a C–C single bond. In addition, an intramolecular hydrogen bond is formed in the benzopyranopyrimidine moiety, which improves the planarity of the whole structure by enhanced π-delocalization.[29] We think that this unique

School of Pharmaceutical Sciences, Sun Yat-sen University, Guangzhou, 510080, People's Republic of China. E-mail: ceshzs@mail.sysu.edu.cn; Fax: 8620-39943056; Tel: 8620-39943056

† Electronic supplementary information (ESI) available. CCDC reference number 798356. For ESI and crystallographic data in CIF or other electronic format see DOI: 10.1039/c0ob00921k

molecular architecture of PBPP offers an attractive template for G-quadruplex ligand design. The PBPPs have compatible structural features including (i) a polycyclic aromatic heterocycle which permits efficient π-stacking interactions with a guanine quartet within a G-quadruplex, and (ii) a rotatable bond between the benzopyranopyrimidine moiety and the phenyl group provides potentially different conformations. However, based on previous reports,[30,31] we hypothesized that the scaffold of PBPP itself alone is probably not sufficient to be an effective G-quadruplex ligand. The addition of two cationic side chains to the PBPP parent core, which could interact with the grooves and loops of the G-quadruplex, may be necessary to enhance its G-quadruplex binding potency and selectivity, as well as its aqueous solubility. Therefore, we synthesized a series of new PBPP derivatives by attaching cationic amino side chain(s) to the benzopyranopyrimidine moiety and/or the phenyl group. Their interactions with telomeric G-quadruplex DNA were then investigated using the fluorescence resonance energy transfer (FRET) method, surface plasmon resonance (SPR), circular dichroism (CD) spectroscopy, and molecular modeling. Besides, their inhibitory effects on telomerase activity were examined using TRAP-LIG, and their cellular effects were evaluated through the measurements of cell senescence and telomere shortening.

Results and discussion

Chemistry

The synthesis of substituted PBPPs followed general pathways as shown in Scheme 1. The PBPPs scaffolds **2a–c** were synthesized according to a previously reported procedure,[26] through ternary condensation of ethyl cyanoacetate, a salicylaldehyde and benzaldehyde in the presence of ammonium acetate. Compounds **2b–c** were refluxed in trifluoroacetic acid to give **3b–c**. Compounds **4a** and **5a** were prepared by mixing **2a** with an excess of the corresponding dibromoalkane, and the resulting solution was refluxed in anhydrous acetone for 18 h with K_2CO_3 as a catalyst. Reaction of **4a** and **5a** with *N*-methyl piperazine or pyrrolidine in dry CH_3CN under reflux for 6 h yielded compounds **6d**, **7b** and **7d**. Compounds **8d**, **9b**, **9d**, **10a–e**, and **11a–e** were also synthesized following similar procedures using different alkylamines. However, the alkylation step required a shorter time of 5 h, and the alkylation of **3c** with 1,2-dibromoethane should be catalyzed with Cs_2CO_3 instead of K_2CO_3 to afford **4c**. Satisfactory analytical and spectroscopic data were obtained for all of the synthesized compounds. In addition, the planarity of the PBPP scaffold was confirmed by the X-ray structure of compound **6d** (Fig. 2), which is essential for the PBPP to partake in π–π stacking with G-quartets. Moreover, the width of the putative stacking portion of the molecule (11.1 Å) was closely related to the dimensions of the G-quadruplex (10.8–13.0 Å) structure, and may be unfavorable for its interaction with duplex DNA which offers a distance of only 5.2–7.3 Å.[20] This structural feature may be important for its selectivity for G-quadruplex over duplex DNA.

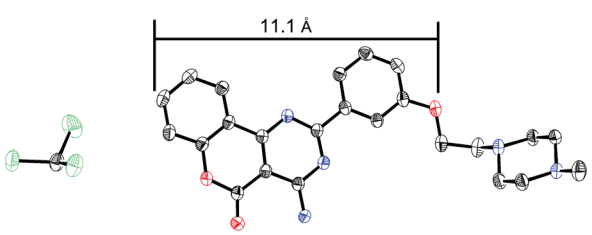

Fig. 2 ORTEP drawing of **6d** with $CDCl_3$. Colors of the atoms: carbon, black; nitrogen, blue; chloride, green; oxygen, red. Hydrogen atoms were omitted for clarity. Drawings were prepared using ORTEP-3 software.[32]

Studies of telomeric G-quadruplex binding and selectivity with FRET assays

The stabilization activity and selectivity of the derivatives to telomeric G-quadruplex DNA were studied using FRET melting experiments[33–35] with F21T and F10T, and the quindoline derivative SYUIQ-5 previously reported by our group[24] was used as a reference compound. F21T (5′-FAM-d(GGG[TTAGGG]$_3$)-TAMRA-3′) represents the human telomeric DNA sequence, while F10T (5′-FAM-dTATAGCTATA-HEG-TATAGCTATA-TAMRA-3′) is a self-complementary duplex DNA hairpin.

The results of the FRET melting experiments (Table 1) indicated that the disubstituted series (**10a–e** and **11a–e**) had a wide range of telomeric G-quadruplex DNA stabilizing activity ranging from 3.8 to 16.5 °C, and the activity of some compounds (**10a–b**, **10e**, **11a–b**) is comparable to that of the quindoline derivative SYUIQ-5. In comparison, all six mono substituted derivatives (**6d–9d**, **7b** and **9b**) had very low G-quadruplex stabilizing properties, which proved our hypothesis that two cationic side chains are important for strong G-quadruplex interactions. For disubstituted compounds, alterations of the basic terminus of the side chains gave the pyrrolidino derivatives (**10b**, **11b**), which had the highest activity for the stabilization of G-quadruplex DNA, while the *N*-methylpiperazino functionality (ΔT_m values of 8.9 and 3.8 °C for **10d** and **11d** respectively) was found to be detrimental to G-quadruplex stabilization. Interestingly, replacement of *N*-methylpiperazino with *N*-2-hydroxyethylpiperazino significantly improved the stabilization property with the ΔT_m values of 14.1 and 8.7 °C for **10e** and **11e** respectively, while **10c** with the piperidino ligand had a relatively low ΔT_m value. Compounds **11a–c** with side chains of the same length ($n = 3$) displayed higher ΔT_m values than compounds **10a–c** with shorter side chains ($n = 2$). In contract, compounds **11d–e** ($n = 3$) exhibited lower ΔT_m values than **10d–e** ($n = 2$). Some further experimental data are necessary for the explanation of these results.

As shown in Table 1, the derivatives had a rather weak effect on the thermal stability of the duplex DNA F10T ($\Delta T_m \leq 1$ °C), suggesting their poor binding to the duplex DNA.[23,36] To further confirm their binding selectivity for G-quadruplex DNA over duplex DNA, compounds **10a–e** and **11a–e** with two cationic side chains were studied with a FRET-based competition assay (Fig. 3), and their G-quadruplex stabilizing activity was tested with a nonfluorescent duplex DNA competitor (ds26).[36,37] In these experiments, the labeled oligonucleotide F21T was melted in the presence of excess ds26 (15 and 50-fold excess). The results clearly indicated a high level of stabilization of the G-quadruplex by these compounds, which was only slightly affected in the presence of 50-fold competitor ds26. The results also showed that these compounds had high selectivity for G-quadruplex DNA over duplex DNA, which may be due to their large planar scaffold and two cationic amino side chains. The above results demonstrated that the PBPP derivatives bearing two cationic side chains are a

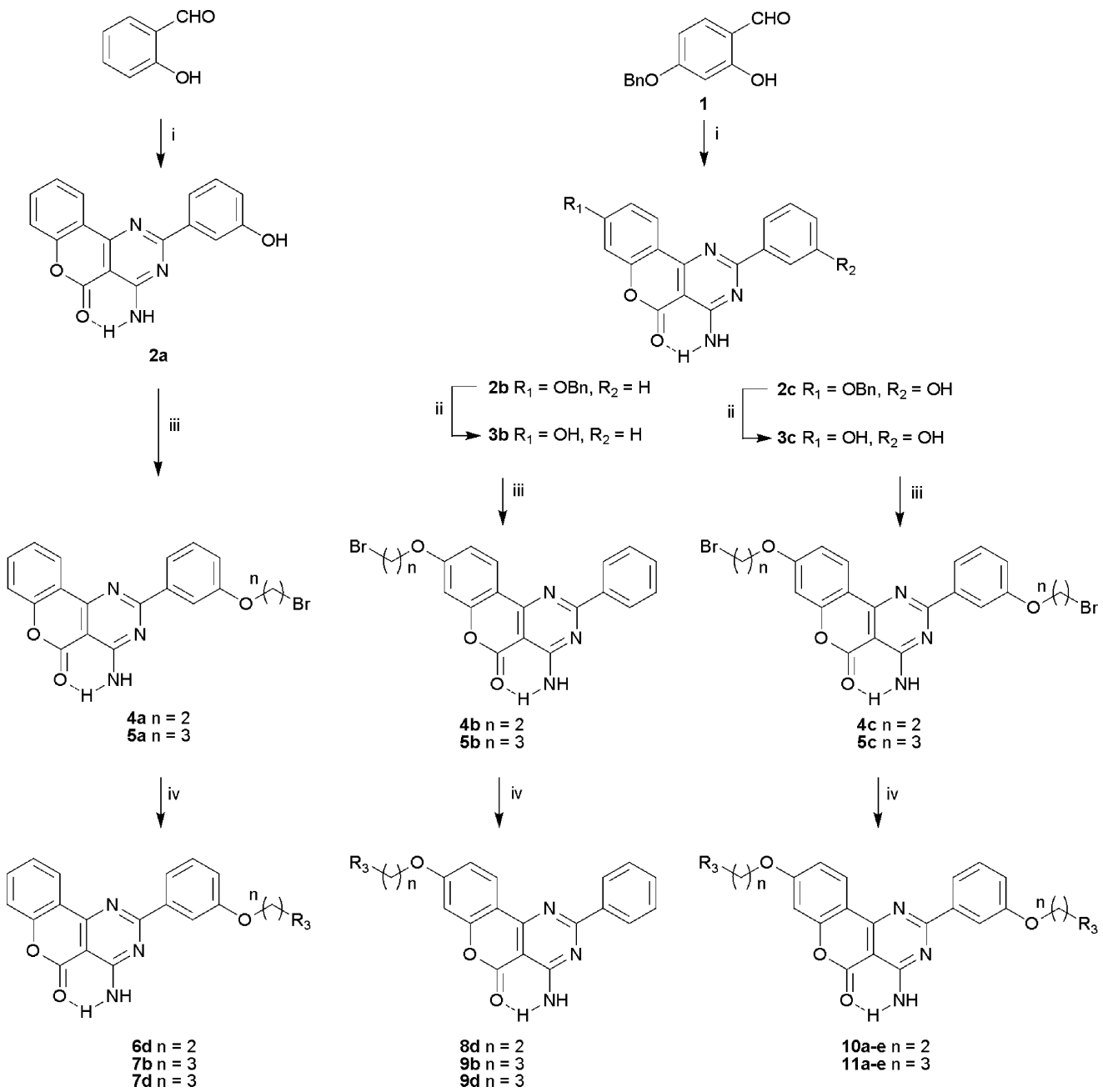

Compd.	a	b	c	d	e
R_3	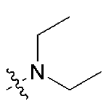	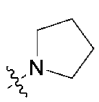	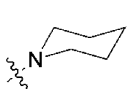	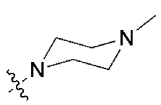	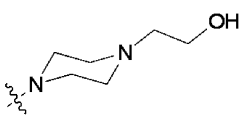

Scheme 1 Synthesis of PBPP derivatives. Reagents: (i) benzaldehydes, ethyl cyanoacetate, ammonium acetate, EtOH (reflux); (ii) TFA (reflux); (iii) 1,2-dibromoethane or 1,3-dibromopropane, K_2CO_3 or Cs_2CO_3, acetone (reflux); (iv) substituted alkylamine, K_2CO_3, CH_3CN (reflux).

Table 1 G-Quadruplex stabilization (ΔT_m) potential obtained from FRET-melting and equilibrium binding constants (K_D) measured with SPR

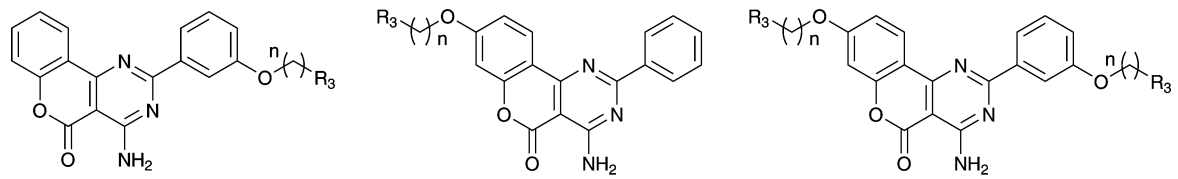

A **B** **C**

Compound	Series	n	R_3	FRET (ΔT_m/°C)[a]		SPR (K_D/μM)	
				F21T	F10T	G4	duplex
6d	A	2	*N*-methylpiperazino	0.5	0.2	—[b]	nd[c]
7b	A	3	pyrrolidino	1.4	0.1	—[b]	—[b]
7d	A	3	*N*-methylpiperazino	1.1	0.2	—[b]	nd[c]
8d	B	2	*N*-methylpiperazino	0.7	0.0	—[b]	nd[c]
9b	B	3	pyrrolidino	1.6	0.1	—[b]	—[b]
9d	B	3	*N*-methylpiperazino	0.5	0.0	—[b]	nd[c]
10a	C	2	diethylamino	12.7	0.7	4.6	—[b]
10b	C	2	pyrrolidino	14.7	1.0	2.9	—[b]
10c	C	2	piperidino	5.7	0.1	7.9	—[b]
10d	C	2	*N*-methylpiperazino	8.9	0.5	18.0	—[b]
10e	C	2	*N*-2-hydroxyethylpiperazino	14.1	0.6	4.2	—[b]
11a	C	3	diethylamino	15.5	0.5	8.6	—[b]
11b	C	3	pyrrolidino	16.5	0.4	4.5	—[b]
11c	C	3	piperidino	10.0	0.6	5.8	—[b]
11d	C	3	*N*-methylpiperazino	3.8	0.3	21.0	—[b]
11e	C	3	*N*-2-hydroxyethylpiperazino	8.7	0.7	6.3	—[b]
SYUIQ5	—	—	—	10.2	5.5	nd[c]	nd[c]

[a] $\Delta T_m = T_m$ (DNA + ligand) – T_m (DNA). ΔT_m values of 0.2 μM F21T or F10T incubated with 1.0 μM compound in the presence of 60 mM KCl. [b] No significant binding was found for addition of up to 20 μM ligand, which might indicate no specific interactions between the ligand and the DNA. [c] Not determined.

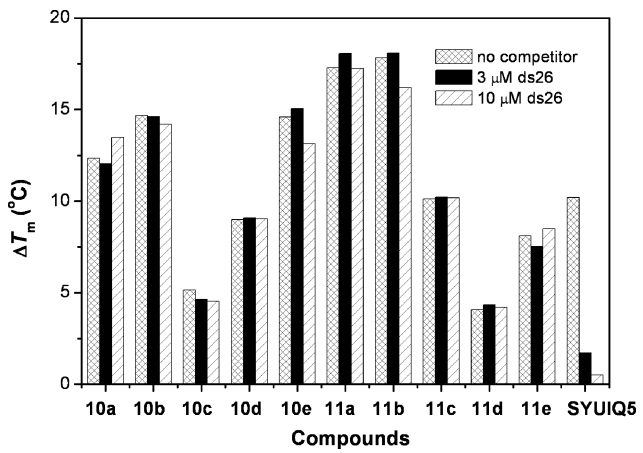

Fig. 3 Competitive FRET results for disubstituted PBPP derivatives and SYUIQ5 (1 μM), without (grid) and with 15-fold (3 μM, black) or 50-fold (10 μM, slash) excess of duplex DNA competitor (ds26). The concentration of F21T was 0.2 μM.

new class of potent and highly selective G-quadruplex binding ligands.

Studies of telomeric G-quadruplex binding and selectivity with surface plasmon resonance (SPR)

The equilibrium constants for the binding of the synthesized compounds to G-quadruplex DNA were determined using SPR with biotinylated telomeric DNA attached to a streptavidin-coated sensor chip.[38,39] A range of concentrations of compounds were injected simultaneously to the immobilized telomeric DNA and the blank reference. The binding constants were determined using equilibrium analysis as shown in Table 1. The binding constants of the disubstituted compounds to telomeric G-quadruplex fell into a wide range (K_D, 2.9–21.0 μM), while no obvious binding was observed using SPR for mono substituted compounds even at a concentration of 20 μM, which was consistent with very low ΔT_m values obtained from FRET melting. These results further confirmed the importance of the disubstitution for the binding of PBPP derivatives to the telomeric G-quadruplex.

Both FRET and SPR experimental results indicated that the pyrrolidino basic group of **10b** or **11b** was optimal for their interaction with telomeric G-quadruplex DNA, while the introduction of the *N*-methylpiperazino group (**10d** and **11d**) was unfavorable for the binding interaction. The replacement of *N*-methylpiperazino with *N*-2-hydroxyethylpiperazino gave increased ΔT_m values. SPR curves for the binding of telomeric G-quadruplex DNA with **10b**, **10d** and **10e** are compared as shown in Fig. 4, and SPR sensorgrams are shown in Fig. S1 (ESI†). It should be noted that some results from SPR experiments are not exactly consistent with those from FRET experiments. For example, compound **10c** showed a moderate binding affinity with a K_D of 7.9 μM measured with SPR, but had a relatively low ΔT_m value. SPR measurements indicated that the side chain length $n = 2$ was better for the interaction, while FRET assays showed that the side chain length $n = 3$ was favored.

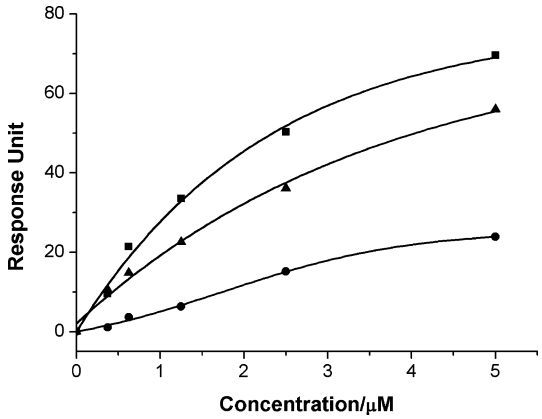

Fig. 4 SPR curves for the binding of **10b** (■), **10d** (●), and **10e** (▲) to human telomeric G-quadruplex DNA; running buffer, 50 mM Tris-HCl, pH 7.2, 100 mM KCl.

On the other hand, incubation of these compounds with duplex DNA immobilized on the chips showed either no significant or non-specific binding interactions, which prevented a determination of their binding affinity. This might indicate that the disubstituted derivatives had selectivity for G-quadruplex DNA, which was in good agreement with our FRET data.

Studies of telomeric G-quadruplex binding and selectivity with circular dichroism (CD)

Circular dichroism (CD) spectroscopy is a well-established method for determining the structural type of G-quadruplex DNA and the effect of ligand binding on quadruplex structures.[40] The interaction of the disubstituted PBPP derivatives with telomeric DNA was further studied with this method. In the presence of 100 mM K^+, the CD spectrum of HTG21 in the absence of any compound showed a major positive band at 291 nm, a shoulder at around 270 nm, a small positive band at 255 nm and a minor negative band near 234 nm. This indicated a mixture of antiparallel and parallel conformations, possibly including hybrid forms as well.[39,40] As shown in Fig. 5a, upon the addition of compound **11b** (5 molar equivalents of HTG21) to the above solution, the CD spectrum significantly changed, with dramatic enhancement of the positive bands near 291 and 270 nm, and remarkable attenuation of the band at 255 nm. Similar results were obtained upon addition of **11d**, but with less significant changes. When adding the same amount of **7b**, the attenuation also occurred for the band at 255 nm, but the bands at 291 and 270 nm showed little change. These results are consistent with those obtained from other experiments in the present study.

In order to further study the binding interaction, CD spectra of HTG21 (5 μM) were also recorded in the presence of increasing concentrations of compound **11b** (2.5–25 μM, corresponding to 0.5–5 equiv of compound **11b**) (Fig. 5b). The band with maximum at 291 nm significantly increased and shifted toward 288 nm, while the shoulder at 270 nm was also gradually enhanced and merged into the band at 288 nm. In the meantime, the small positive band at 255 nm gradually decreased. The changes in the CD spectra were obviously concentration dependent, but we were not able to figure out particular conformational changes occurring for HTG21 based on the present information.

Molecular modeling studies

In order to understand the nature of the interactions between PBPP derivatives and the telomeric G-quadruplex, molecular docking experiments and molecular dynamics (MD) simulations were carried out. Compound **11b** was selected in this study as the best binding ligand, while compound **7b** was used as a poor binding ligand for comparison. The propeller G-quadruplex crystal structure was taken as a template for the modeling studies, because it should be a biologically relevant form for ligand binding.[41] Our results from clustering analysis of molecular docking indicated that compound **11b** preferred to bind on the 3′ G-quartet surface, and the terminal side chains with protonated amino groups were directed into the grooves and interacted with the phosphate diester backbone. This can be explained by the following two reasons: (i) the 3′ G-quartet surface is polar and interaction with ligands containing cationic side chains is favorable, and (ii) the grooves generated with TTA loops on this side are much more accessible to the side chains of the ligands.[42] This complex obtained from the docking experiment was then used for subsequent MD simulation studies.

The MD simulation results clearly showed that the two phenyl groups of the planar aromatic scaffold effectively stacked on the 3′ G-quartet surface, and fixed the pyrimidine ring of the

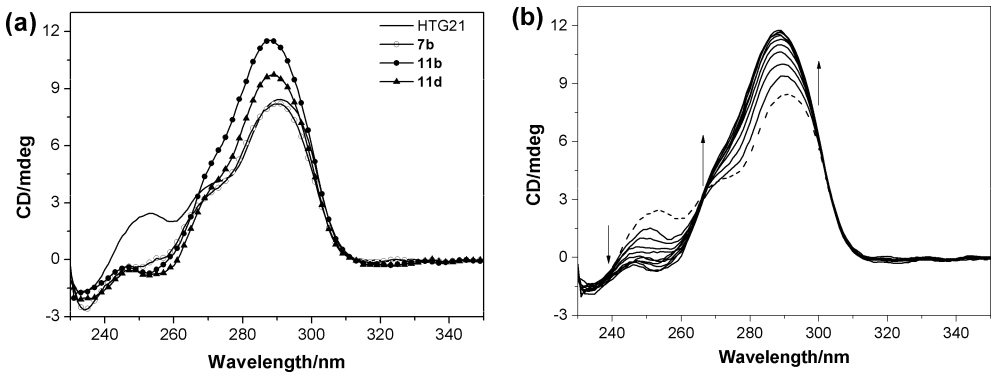

Fig. 5 CD spectra of HTG21 in 10 mM Tris-HCl buffer, pH 7.2, 100 mM KCl. (a) CD spectra of HTG21 (solid line), and HTG21 in the presence of 5 equivalents of **7b** (○), **11b** (●) and **11d** (▲), respectively. (b) CD titration spectra of HTG21 (5 μM) at increasing concentrations of **11b** (0–5 mol equiv; dashed line indicated HTG21 in the absence of **11b**).

Table 2 Telomerase inhibition by PBPP derivatives in cell-free assay

	7b	11b	11d	11e
IC_{50} (μM)	>40	3.4	33.5	10.8

benzopyranopyrimidine moiety over the negatively charged carbonyl channel of the G-quadruplex. The two positively-charged side chains were properly oriented and directed into the DNA groove towards the negatively charged phosphate diester backbone, and formed electrostatic interactions and hydrogen bonds (Fig. 6a). The binding free energy of the telomeric G-quadruplex complexed with compound **11b** was estimated to be −19.5 kcal mol^{-1} by the MM-PBSA approach. The modeling study showed that compound **7b** had a similar binding mode (Fig. 6b) to compound **11b**, however, its estimated binding free energy (−10.4 kcal mol^{-1}) was much higher than that of **11b**, suggesting again the essential role of double side chains for G-quadruplex binding.

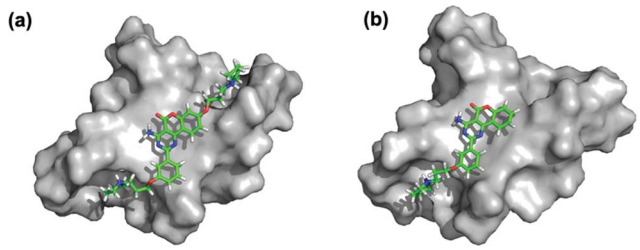

Fig. 6 Top view of compound (a) **11b** and (b) **7b** forming π–π stacking interactions with the 3′ G-quartet. The ligand side chain(s) is/are lying in the grooves formed by the TTA loops. Pictures are generated with PyMOL.[43]

Telomerase inhibition

The ability of PBPP derivatives to inhibit human telomerase activity was evaluated with a modified TRAP assay. The TRAP-LIG assay provided quantitative measurement of telomerase inhibition by the small molecules. Considering the compounds might interact with the extension reaction products thus interfering with the PCR step, the ligands were removed after incubation with the enzyme and prior to the amplification step.[44] In the experiments, solutions of derivatives were added to the telomerase reaction mixture containing extracts from A549 human lung adenocarcinoma cell line, and their IC_{50} values were obtained as shown in Table 2. It was found that the inhibitory effects of disubstituted PBPP derivatives on telomerase activity were significantly enhanced when compared to those of the mono substituted derivative **7b**. Thus, introduction of two positively charged side arms on PBPP could improve its inhibitory activity against telomerase. Compound **11b** was found to have the strongest inhibitory effect to the enzyme.

Short-term cell viability

The short-term cell growth inhibitory activity of the PBPP derivatives was evaluated using the MTT assay for three telomerase-positive cancer cell lines (A549, HepG2 and K562) and one normal cell line (ECV-304) (Table 3). All the tested derivatives had a moderate or significant cytotoxicity on the tested cancer cells, and generally showed strong cell growth inhibition against the A549 cell line. It should be noted that the mono substituted derivatives **7b** and **9b** also showed high cytotoxicity against the cells, although they had little effects on G-quadruplex binding and stabilization, which may be due to other factors. One aim of cancer research is to target cancer cells with certain selectivity over normal cells. Our experimental data showed that some derivatives had moderate selectivity.

Table 3 IC_{50} values (μM) of the disubstituted PBPP derivatives against cancer cells

IC_{50} (μM)	A549	HepG2	K562	ECV-304
7b	9.7	4.4	6.9	5.9
9b	7.3	22.7	8.5	12.5
10a	2.3	11.2	7.8	15.3
10b	2.3	40.1	14.5	4.1
10c	2.4	11.2	5.5	6.3
10d	3.8	30.4	16.5	15.8
10e	4.0	24.9	13.0	14.0
11a	2.5	6.0	4.7	7.0
11b	2.2	2.1	5.0	15.5
11c	2.2	42.0	4.5	5.8
11d	2.3	2.4	8.8	13.2
11e	1.6	45.3	7.5	14.5

Senescence induced by PBPP derivative 11b

Since compound **11b** was found to be the most promising compound as a telomerase inhibitor and telomeric G-quadruplex binding ligand in the above studies, the following further in-depth experimental studies were carried out only for this particular compound. Results of short-term cell viability determined with the MTT assay showed that the PBPP derivatives had potent inhibitory effects for cancer cells. These results prompted us to further investigate the long-term effects of these derivatives. To avoid acute cytotoxicity and other nonspecific events that could lead to difficulty in the interpretation of results, the effects of compound **11b** at subcytotoxic concentrations (1 and 0.25 μM) on K562 cells were evaluated through long-term exposure. Treatment of K562 cells with 1 μM compound **11b** resulted in a significant inhibitory effect. In the presence of even 0.25 μM compound **11b**, the population doubling time increased substantially compared to that of the control (Fig. 7a).

Morphological examination of the cells in long-term studies showed an increased proportion of enlarged and flattened cells with phenotypic characteristics of senescence.[6,45] These flattened cells were also stained positively for the senescence-associated-galactosidase (SA-β-Gal) activity after continuous treatment with compound **11b** (Fig. 7b, c), and our result showed that compound **11b** induced accelerated senescence of K562 cancer cells.

Telomere shortening by PBPP derivative 11b

Inhibition of telomerase and interaction with telomere G-overhang in cancer cells were predicted to disrupt telomere length maintenance and cause telomeres to erode.[46–48] To investigate whether representative PBPP derivative **11b** could cause telomere shortening, telomere length was evaluated using the telomeric restriction fragment (TRF) length assay (Fig. 8) on leukemia cell K562. The results showed that 1 μM compound **11b** triggered telomere shortening about 1.3 kb for K562 cells, and the telomere shortening was also observed after treatment with 0.25 μM

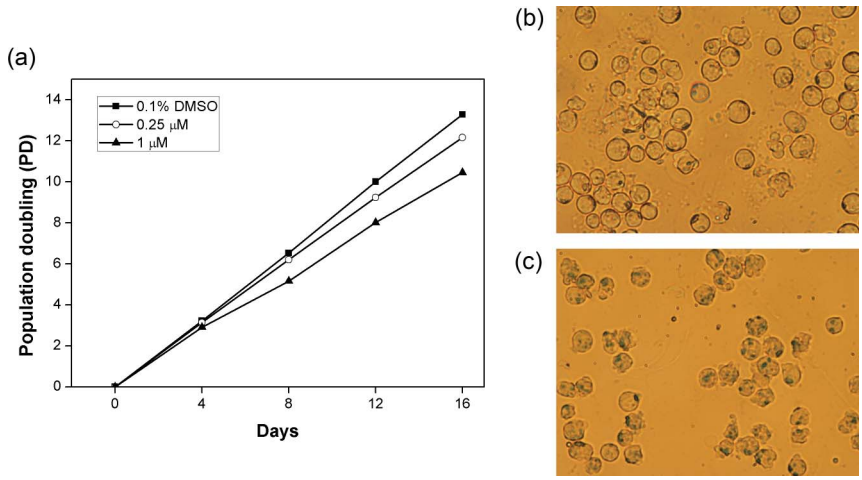

Fig. 7 Senescence induced by compound **11b** on K562 cells. (a) Long-term incubation of K562 with compound **11b** at subcytotoxic concentrations. Expression of SA-β-Gal in K562 cells after treatment with (b) 0.1% DMSO or (c) 1 μM compound **11b** continuously for 16 days.

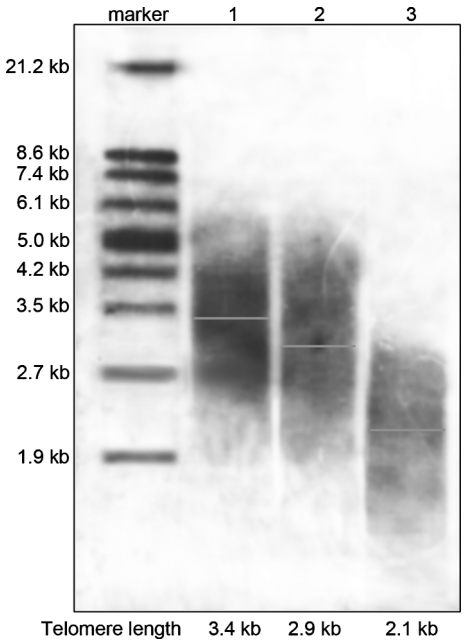

Fig. 8 Effect of PBPP derivative **11b** on telomere length. TRF analysis of K562 cells treated with or without compound **11b** for 16 days. Lane 1, 0.1% DMSO; lane 2, 0.25 μM compound **11b**; lane 3, 1 μM compound **11b**.

compound **11b**. It has been reported that a dysfunctional telomere could activate p53 to initiate cellular senescence or apoptosis to suppress tumorigenesis,[17] and here the induction of senescence by compound **11b** might be due to the shortening of telomere length. This result is consistent with those reported previously for efficient telomeric G-quadruplex ligands and telomerase inhibitors.[48,49] It should be noted that the cellular effect of compound **11b** may not be simply explained through telomeric G-quadruplex interactions or telomerase inhibition. Other possible telomere-independent genomic DNAs such as promoter G-quadruplex could also be the target of this molecule. Nevertheless, compound **11b** as a new selective G-quadruplex ligand, could become a useful lead compound for further development for anticancer therapeutics.

Conclusion

In the present study, we synthesized and studied a novel series of PBPP-based compounds, which showed effective and selective binding to telomeric G-quadruplex DNA. To the best of our knowledge, this is the first time that PBPP derivatives were demonstrated to be strong telomeric G-quadruplex binding ligands. Our experimental results indicated that disubstitution of PBPPs was important for their binding with the G-quadruplex, and the disubstituted PBPP derivatives showed high binding affinity and significant selectivity for G-quadruplex DNA over duplex DNA. The terminal pyrrolidino group was proved to be optimal for G-quadruplex binding. The G-quadruplex-ligand binding mechanism was studied with molecular modeling experiments, which indicated that the ligand stacked on the terminal G-quartet of the G-quadruplex structure with the side chains of the ligand reaching the grooves of the G-quadruplex. Moreover, the disubstituted PBPP derivatives were found to be strong telomerase inhibitors, and long-term incubation of K562 cancer cells with compound **11b** showed a remarkable decrease of cell population accompanied with a shortening of the telomere length, which are consistent with those previously reported for effective telomerase inhibitors and telomeric G-quadruplex ligands. These results shed light on the further design of more potent and selective telomeric G-quadruplex-interactive compounds.

Experimental section

^{1}H and ^{13}C NMR spectra were recorded using TMS as the internal standard in DMSO-d_6 or $CDCl_3$ with a Bruker BioSpin GmbH spectrometer at 400 MHz and 100 MHz, respectively; Mass spectra (MS) were recorded on a Shimadzu LCMS-2010A instrument with an ESI or ACPI mass selective detector, and high resolution mass spectra (HRMS) on Shimadzu LCMS-IT-TOF. Melting points (m.p.) were determined using a SRS-OptiMelt automated melting point instrument without correction. Flash column chromatography was performed with silica gel (200–300 mesh) purchased from Qingdao Haiyang Chemical Co. Ltd. The purities of synthesized compounds were confirmed to be

higher than 95% by analytical HPLC performed with a dual pump Shimadzu LC-20AB system equipped with a Ultimate XB-C18 column (4.6 × 250 mm, 5 μm) and eluted with methanol–water (35 : 65 to 59 : 41) containing 0.1% TFA at a flow rate of 1 mL min^{-1}.

General procedure: Preparation of 6d–9d, 7b, 9b, 10a–e, and 11a–e

To a stirred suspension of compounds **4a–c** or **5a–c** (1 mmol) and anhydrous K_2CO_3 (5 mmol) in dry acetonitrile (50 mL) was added excess alkylamine (5 mmol), and the resulting mixture was heated under reflux for 6 h until the starting material disappeared. The K_2CO_3 was removed through filtration, and the remaining solution was concentrated under reduced pressure. The crude product was purified using flash chromatography with $CHCl_3$–$MeOH/NH_3{\cdot}H_2O$ (50 : 1 : 0.1) as elution solvent to give the desired product.

4-Amino-2-(3-(2-(4-methylpiperazin-1-yl)ethoxy)phenyl)-5*H*-chromeno[4,3-d]pyrimidin-5-one (6d). Compound **4a** was treated with *N*-methylpiperazine following the general procedure to give the desired product **6d** as a white solid with a yield of 29%. m.p. 204–206 °C; ^{1}H NMR (400 MHz, $CDCl_3$) δ 8.65 (dd, J = 7.9, 1.5 Hz, 1H), 8.34 (br d, J = 3.7 Hz, 1H), 8.20–8.15 (m, 1H), 8.12 (dd, J = 2.5, 1.5 Hz, 1H), 7.65 (ddd, J = 8.3, 7.3, 1.7 Hz, 1H), 7.46–7.33 (m, 3H), 7.10 (ddd, J = 8.2, 2.7, 0.9 Hz, 1H), 6.14 (br d, J = 3.8 Hz, 1H), 4.25 (t, J = 5.8 Hz, 2H), 2.90 (t, J = 5.8 Hz, 2H), 2.82–2.40 (m, 8H), 2.32 (s, 3H); ^{13}C NMR (101 MHz, $CDCl_3$) δ 167.25, 163.52, 161.85, 159.88, 158.97, 153.81, 138.42, 133.62, 129.43, 125.75, 124.79, 121.81, 118.57, 117.03, 114.64, 95.97, 66.02, 57.23, 55.06, 53.59, 46.02; HRMS (ESI+) m/z: Calc. for $C_{24}H_{25}N_5O_3$: 432.2036 $[M+H]^+$. Found 432.2030 $[M+H]^+$.

4-Amino-2-(3-(3-(pyrrolidin-1-yl)propoxy)phenyl)-5*H*-chromeno[4,3-d]pyrimidin-5-one (7b). Compound **5a** was treated with pyrrolidine following the general procedure to give the desired product **7b** as a yellow solid with a yield of 49%. m.p. 156–157 °C; ^{1}H NMR (400 MHz, $CDCl_3$) δ 8.53 (dd, J = 7.9, 1.5 Hz, 1H), 8.23 (d, J = 3.9 Hz, 1H), 8.13–8.06 (m, 1H), 8.02 (dd, J = 2.4, 1.5 Hz, 1H), 7.57 (ddd, J = 8.4, 7.3, 1.7 Hz, 1H), 7.39–7.31 (m, 2H), 7.28 (dd, J = 8.3, 0.6 Hz, 1H), 7.05 (ddd, J = 8.2, 2.6, 0.8 Hz, 1H), 6.41 (d, J = 3.9 Hz, 1H), 4.14 (t, J = 6.3 Hz, 2H), 2.70 (t, J = 7.2 Hz, 2H), 2.64–2.52 (m, 4H), 2.15–2.01 (m, 2H), 1.87–1.74 (m, 4H); ^{13}C NMR (101 MHz, $CDCl_3$) δ 167.08, 163.44, 161.74, 159.63, 159.15, 153.70, 138.29, 133.42, 129.29, 125.64, 124.63, 121.53, 118.48, 118.42, 116.88, 114.43, 95.82, 66.39, 54.26, 53.15, 28.90, 23.48. HRMS (ESI+) m/z: Calc. for $C_{24}H_{24}N_4O_3$: 415.1770 $[M - H]^-$. Found 415.1767 $[M - H]^-$.

4-Amino-2-(3-(3-(4-methylpiperazin-1-yl)propoxy)phenyl)-5*H*-chromeno[4,3-d]pyrimidin-5-one (7d). Compound **5a** was treated with *N*-methylpiperazine following the general procedure to give the desired product **7d** as a white solid with a yield of 27%. m.p. 193–195 °C; ^{1}H NMR (400 MHz, $CDCl_3$) δ 8.66 (dd, J = 7.9, 1.6 Hz, 1H), 8.34 (br d, J = 3.5 Hz, 1H), 8.20–8.14 (m, 1H), 8.10 (dd, J = 2.5, 1.5 Hz, 1H), 7.65 (ddd, J = 8.4, 7.3, 1.7 Hz, 1H), 7.46–7.34 (m, 3H), 7.08 (ddd, J = 8.2, 2.6, 0.9 Hz, 1H), 6.14 (br d, J = 3.7 Hz, 1H), 4.15 (t, J = 6.3 Hz, 2H), 2.76–2.45 (m, 10H), 2.33 (s, 3H), 2.12–1.99 (m, 2H); ^{13}C NMR (101 MHz, $CDCl_3$) δ 167.32, 163.53, 161.84, 159.88, 159.20, 153.83, 138.42, 133.60, 129.42, 125.74, 124.77, 121.65, 118.55, 118.39, 117.03, 114.69, 95.96, 66.35, 55.12, 54.98, 52.98, 45.86, 26.75; HRMS (ESI+) m/z: Calc. for $C_{25}H_{27}N_5O_3$: 446.2192 $[M+H]^+$. Found 446.2191 $[M+H]^+$.

4-Amino-8-(2-(4-methylpiperazin-1-yl)ethoxy)-2-phenyl-5*H*-chromeno[4,3-d]pyrimidin-5-one (8d). Compound **4b** was treated with *N*-methylpiperazine following the general procedure to give the desired product **8d** as a white solid with a yield of 10%. m.p. 190–192 °C; ^{1}H NMR (400 MHz, $CDCl_3$) δ 8.59–8.52 (m, 3H), 8.28 (br s, 1H), 7.55–7.49 (m, 3H), 6.98 (dd, J = 8.9, 2.4 Hz, 1H), 6.83 (d, J = 2.3 Hz, 1H), 6.02 (br s, 1H), 4.20 (t, J = 5.7 Hz, 2H), 2.88 (t, J = 5.7 Hz, 2H), 2.68 (s, 4H), 2.55 (s, 4H), 2.34 (s, 3H); ^{13}C NMR (101 MHz, $CDCl_3$) δ 167.55, 163.62, 163.41, 162.17, 159.91, 155.49, 137.20, 131.72, 129.11, 128.44, 126.97, 113.38, 111.87, 101.46, 94.63, 66.69, 56.84, 54.95, 53.41, 45.85; HRMS (ESI+) m/z: Calc. for $C_{24}H_{25}N_5O_3$: 432.2036 $[M+H]^+$. Found 432.2020 $[M+H]^+$.

4-Amino-2-phenyl-8-(3-(pyrrolidin-1-yl)propoxy)-5*H*-chromeno[4,3-d]pyrimidin-5-one (9b). Compound **5b** was treated with pyrrolidine following the general procedure to give the desired product **9b** as a yellow solid with a yield of 47%. m.p. 172–173 °C. ^{1}H NMR (400 MHz, $CDCl_3$) δ 8.56 (dd, J = 7.9, 1.6 Hz, 2H), 8.46 (d, J = 8.8 Hz, 1H), 8.24 (d, J = 3.2 Hz, 1H), 7.60–7.44 (m, 3H), 6.91 (dd, J = 8.8, 2.4 Hz, 1H), 6.74 (d, J = 2.3 Hz, 1H), 6.35 (d, J = 3.2 Hz, 1H), 4.11 (t, J = 6.3 Hz, 2H), 2.69 (t, J = 7.3 Hz, 2H), 2.64–2.50 (m, 4H), 2.12–2.00 (m, 2H), 1.90–1.74 (m, 4H); ^{13}C NMR (101 MHz, $CDCl_3$) δ 167.31, 163.61, 163.54, 162.12, 159.74, 155.37, 137.22, 131.61, 129.05, 128.38, 126.73, 113.18, 111.45, 101.19, 66.83, 54.21, 52.76, 28.52, 23.47. HRMS (ESI+) m/z: Calc. for $C_{24}H_{24}N_4O_3$: 415.1770 $[M - H]^-$. Found 415.1774 $[M - H]^-$.

4-Amino-8-(3-(4-methylpiperazin-1-yl)propoxy)-2-phenyl-5*H*-chromeno[4,3-d]pyrimidin-5-one (9d). Compound **5b** was treated with *N*-methylpiperazine following the general procedure to give the desired product **9d** as a white solid with a yield of 34%. m.p. 208–209 °C; ^{1}H NMR (400 MHz, $CDCl_3$) δ 8.56 (dd, J = 7.9, 1.7 Hz, 2H), 8.52 (d, J = 8.8 Hz, 1H), 8.27 (br s, 1H), 7.56–7.46 (m, 3H), 6.95 (dd, J = 8.8, 2.4 Hz, 1H), 6.81 (d, J = 2.3 Hz, 0H), 6.05 (br s, 1H), 4.11 (t, J = 6.3 Hz, 1H), 2.73–2.36 (m, 5H), 2.31 (s, 2H), 2.07–1.99 (m, 1H); ^{13}C NMR (101 MHz, $CDCl_3$) δ 167.48, 163.72, 163.59, 162.19, 159.91, 155.51, 137.21, 131.69, 129.09, 128.43, 126.87, 113.34, 111.61, 101.28, 94.54, 66.93, 55.14, 54.85, 53.21, 46.03, 26.54; HRMS (ESI+) m/z: Calc. for $C_{25}H_{27}N_5O_3$: 446.2192 $[M+H]^+$. Found 446.2178 $[M+H]^+$.

4-Amino-8-(2-(diethylamino)ethoxy)-2-(3-(2-(diethylamino)-ethoxy)phenyl)-5*H*-chromeno[4,3-d]pyrimidin-5-one (10a). Compound **4c** was treated with *N*,*N*-diethylamine following the general procedure to give the desired product **10a** as a pale yellow solid with a yield of 18%. m.p. 94–96 °C; ^{1}H NMR (400 MHz, $CDCl_3$) δ 8.37 (d, J = 8.8 Hz, 1H), 8.17 (br s, 1H), 8.07 (d, J = 7.6 Hz, 1H), 8.02 (s, 1H), 7.33 (t, J = 7.9 Hz, 1H), 7.03 (dd, J = 8.0, 1.7 Hz, 1H), 6.87 (dd, J = 8.8, 2.1 Hz, 1H), 6.69 (d, J = 1.9 Hz, 1H), 6.39 (br s, 1H), 4.18 (t, J = 6.1 Hz, 2H), 4.07 (t, J = 5.7 Hz, 2H), 2.96 (t, J = 6.0 Hz, 2H), 2.89 (t, J = 5.9 Hz, 2H), 2.72 (q, J = 14.3, 7.2 Hz, 4H), 2.66 (q, J = 14.4, 7.2 Hz, 4H), 1.12 (t, J = 8.0 Hz, 6H), 1.08 (t, J = 8.0 Hz, 6H); ^{13}C NMR (101 MHz, $CDCl_3$) δ 166.90, 163.42, 163.31, 162.00, 159.58, 158.80, 155.26, 138.54, 129.29, 126.73, 121.70, 118.37, 114.27, 113.14, 111.53, 101.19, 94.43, 67.12, 66.17,

51.64, 51.49, 47.81, 47.70, 11.67, 11.48; HRMS (ESI+) *m/z*: Calc. for $C_{27}H_{39}N_5O_4$: 520.2900 $[M+H]^+$. Found 520.2918 $[M+H]^+$.

4-Amino-8-(2-(pyrrolidin-1-yl)ethoxy)-2-(3-(2-(pyrrolidin-1-yl)-ethoxy)phenyl)-5*H*-chromeno[4,3-d]pyrimidin-5-one (10b). Compound **4c** was treated with pyrrolidine following the general procedure to give the desired product **10b** as a pale yellow solid with a yield of 31%. m.p. 124–125 °C; ^{1}H NMR (400 MHz, $CDCl_3$) δ 8.44 (t, J = 8.8 Hz, 1H), 8.22 (br d, J = 4.0 Hz, 1H), 8.11 (d, J = 7.8 Hz, 1H), 8.08 (s, 1H), 7.37 (t, J = 7.9 Hz, 1H), 7.08 (dd, J = 8.2, 1.8 Hz, 1H), 6.94 (dd, J = 8.9, 2.4 Hz, 1H), 6.76 (d, J = 2.3 Hz, 1H), 6.32 (br d, J = 4.0 Hz, 1H), 4.24 (t, J = 5.9 Hz, 2H), 4.17 (t, J = 5.8 Hz, 2H), 2.99 (t, J = 5.9 Hz, 2H), 2.94 (t, J = 5.8 Hz, 2H), 2.70 (t, J = 6.8 Hz, 4H), 2.67 (t, J = 6.9 Hz, 5H), 1.91–1.84 (m, 4H), 1.84–1.77 (m, 4H); ^{13}C NMR (101 MHz, $CDCl_3$) δ 167.04, 163.47, 163.37, 162.08, 159.67, 158.92, 155.31, 138.54, 129.30, 126.81, 121.68, 118.39, 114.52, 113.25, 111.62, 101.26, 94.49, 67.67, 66.98, 55.09, 54.75, 54.72, 23.51; HRMS (ESI+) *m/z*: Calc. for $C_{29}H_{33}N_5O_4$: 516.2611 $[M+H]^+$. Found 516.2610 $[M+H]^+$.

4-Amino-8-(2-(piperidin-1-yl)ethoxy)-2-(3-(2-(piperidin-1-yl)-ethoxy)phenyl)-5*H*-chromeno[4,3-d]pyrimidin-5-one (10c). Compound **4c** was treated with piperidine following the general procedure to give the desired product **10c** as a pale yellow solid with a yield of 35%. m.p. 127–129 °C; ^{1}H NMR (400 MHz, $CDCl_3$) δ 8.52 (d, J = 8.8 Hz, 1H), 8.29 (br d, J = 3.4 Hz, 1H), 8.17 (d, J = 7.8 Hz, 1H), 8.11 (s, 1H), 7.41 (t, J = 7.9 Hz, 1H), 7.09 (dd, J = 8.0, 2.1 Hz, 1H), 6.98 (dd, J = 8.9, 2.3 Hz, 1H), 6.82 (d, J = 2.3 Hz, 1H), 6.05 (br d, J = 4.3 Hz, 1H), 4.33 (t, J = 5.7 Hz, 2H), 4.23 (t, J = 5.8 Hz, 2H), 2.96 (t, J = 5.3 Hz, 2H), 2.86 (t, J = 5.8 Hz, 2H), 2.69 (s, 4H), 2.58 (s, 4H), 1.81–1.68 (m, J = 12.3, 7.0 Hz, 4H), 1.69–1.59 (m, J = 11.0, 5.5 Hz, 4H), 1.56–1.41 (m, 4H); ^{13}C NMR (101 MHz, $CDCl_3$) δ 165.90, 162.40, 162.25, 161.00, 158.54, 157.83, 154.23, 137.51, 128.26, 125.70, 120.65, 117.31, 113.45, 112.16, 110.52, 100.18, 93.41, 65.45, 64.78, 56.92, 56.63, 54.09, 54.03, 24.80, 24.77, 23.10, 23.09; HRMS (ESI+) *m/z*: Calc. for $C_{31}H_{37}N_5O_4$: 544.2924 $[M+H]^+$. Found 544.2926 $[M+H]^+$.

4-Amino-8-(2-(4-methylpiperazin-1-yl)ethoxy)-2-(3-(2-(4-methylpiperazin-1-yl)ethoxy)phenyl)-5*H*-chromeno[4,3-d]pyrimidin-5-one (10d). Compound **4c** was treated with *N*-methylpiperazine following the general procedure to give the desired product **10d** as a pale yellow solid with a yield of 45%. m.p. 141–142 °C; ^{1}H NMR (400 MHz, $CDCl_3$) δ 8.45 (d, J = 8.8 Hz, 1H), 8.23 (br d, J = 4.3 Hz, 1H), 8.12 (d, J = 7.8 Hz, 1H), 8.08–8.02 (m, J = 2.3, 1.5 Hz, 1H), 7.39 (t, J = 7.9 Hz, 1H), 7.06 (dd, J = 7.8, 2.2 Hz, 1H), 6.91 (dd, J = 8.8, 2.4 Hz, 1H), 6.75 (d, J = 2.3 Hz, 1H), 6.41 (br d, J = 4.3 Hz, 1H), 4.13 (t, J = 6.3 Hz, 2H), 4.07 (t, J = 6.3 Hz, 2H), 2.75–2.41 (m, 20H), 2.31 (s, 3H), 2.30 (s, 3H), 2.08–1.98 (m, 4H); ^{13}C NMR (101 MHz, $CDCl_3$) δ 167.00, 163.46, 163.25, 162.04, 159.64, 158.87, 155.30, 138.56, 129.34, 126.80, 121.74, 118.36, 114.55, 113.25, 111.65, 101.24, 94.51, 66.49, 65.92, 57.21, 56.86, 55.00, 54.96, 53.57, 53.56, 45.99; HRMS (ESI+) *m/z*: Calc. for $C_{31}H_{39}N_7O_4$: 574.3142 $[M+H]^+$. Found 574.3155 $[M+H]^+$.

4-Amino-8-(2-(4-(2-hydroxyethyl)piperazin-1-yl)ethoxy)-2-(3-(2-(4-(2-hydroxyethyl)piperazin-1-yl)ethoxy)phenyl)-5*H*-chromeno[4,3-d]pyrimidin-5-one (10e). Compound **4c** was treated with *N*-(2-hydroxyethyl)piperazine following the general procedure to give the desired product **10e** as a pale yellow solid with a yield of 19%. m.p. 156–158 °C; ^{1}H NMR (400 MHz, $CDCl_3$) δ 8.49 (d, J = 8.8 Hz, 1H), 8.26 (br d, J = 4.0 Hz, 1H), 8.15 (d, J = 7.7 Hz, 1H), 8.09 (s, 1H), 7.40 (t, J = 7.9 Hz, 1H), 7.08 (dd, J = 8.1, 2.3 Hz, 1H), 6.96 (dd, J = 8.9, 2.3 Hz, 1H), 6.80 (d, J = 2.3 Hz, 1H), 6.16 (br d, J = 4.2 Hz, 1H), 4.24 (t, J = 5.7 Hz, 2H), 4.18 (t, J = 5.6 Hz, 2H), 3.63 (t, J = 5.4 Hz, 4H), 2.89 (t, J = 4.2 Hz, 2H), 2.86 (t, J = 4.1 Hz, 2H), 2.70–2.34 (m, 21H); ^{13}C NMR (101 MHz, $CDCl_3$) δ 166.13, 162.47, 162.31, 161.08, 158.75, 157.88, 154.38, 137.57, 128.40, 125.89, 120.77, 117.38, 113.60, 112.30, 110.71, 100.33, 93.57, 76.33, 76.21, 76.01, 75.69, 65.55, 64.95, 58.25, 58.22, 56.71, 56.20, 55.85, 52.67, 52.63, 51.78, 51.73; HRMS (ESI+) *m/z*: Calc. for $C_{33}H_{43}N_7O_6$: 634.3353 $[M+H]^+$. Found 634.3378 $[M+H]^+$.

4-Amino-8-(3-(diethylamino)propoxy)-2-(3-(3-(diethylamino)-propoxy)phenyl)-5*H*-chromeno[4,3-d]pyrimidin-5-one (11a). Compound **5c** was treated with *N*,*N*-diethylamine following the general procedure to give the desired product **11a** as a light brown solid with a yield of 15%. m.p. 91–92 °C; ^{1}H NMR (400 MHz, $CDCl_3$) δ 8.52 (d, J = 8.9 Hz, 1H), 8.27 (br s, 1H), 8.15 (d, J = 7.8 Hz, 1H), 8.10 (s, 1H), 7.40 (t, J = 7.9 Hz, 1H), 7.08 (dd, J = 8.1, 1.8 Hz, 1H), 6.96 (dd, J = 8.8, 2.4 Hz, 1H), 6.82 (d, J = 2.3 Hz, 1H), 6.03 (br s, 1H), 4.21–4.04 (m, 4H), 2.70 (t, J = 7.4 Hz, 2H), 2.64 (t, 2H), 2.63–2.51 (m, 8H), 2.05–1.93 (m, 4H), 1.08 (t, J = 4.7 Hz, 6H), 1.05 (t, J = 4.7 Hz, 6H); ^{13}C NMR (101 MHz, $CDCl_3$) δ 167.27, 163.76, 163.51, 162.17, 159.85, 159.23, 155.48, 138.58, 129.34, 126.85, 121.54, 118.33, 114.61, 113.28, 111.51, 101.27, 94.54, 67.02, 66.52, 49.47, 49.18, 47.02, 47.00, 26.98, 26.86, 11.75, 11.63; HRMS (ESI+) *m/z*: Calc. for $C_{31}H_{41}N_5O_4$: 548.3237 $[M+H]^+$. Found 548.3248 $[M+H]^+$.

4-Amino-8-(3-(pyrrolidin-1-yl)propoxy)-2-(3-(3-(pyrrolidin-1-yl)propoxy)phenyl)-5*H*-chromeno[4,3-d]pyrimidin-5-one (11b). Compound **5c** was treated with pyrrolidine following the general procedure to give the desired product **11b** as a light brown solid with a yield of 33%. m.p. 136–138 °C; ^{1}H NMR (400 MHz, $CDCl_3$) δ 8.38 (d, J = 8.8 Hz, 1H), 8.17 (br d, J = 4.2 Hz, 1H), 8.11 (d, J = 7.8 Hz, 1H), 8.04 (s, 1H), 7.38 (t, J = 7.9 Hz, 1H), 7.06 (dd, J = 7.4, 2.6 Hz, 1H), 6.85 (dd, J = 8.8, 2.4 Hz, 1H), 6.67 (d, J = 2.3 Hz, 1H), 6.60 (br d, J = 4.1 Hz, 1H), 4.15 (t, J = 6.3 Hz, 2H), 4.07 (t, J = 6.2 Hz, 2H), 2.72 (t, 2H), 2.68 (t, 2H), 2.65–2.51 (m, 8H), 2.14–2.00 (m, 4H), 1.88–1.72 (m, 8H); ^{13}C NMR (101 MHz, $CDCl_3$) δ 166.97, 163.50, 163.46, 162.04, 159.56, 159.12, 155.27, 138.60, 129.28, 126.70, 121.55, 118.28, 114.41, 113.03, 111.39, 101.12, 94.36, 77.36, 77.25, 77.04, 76.73, 66.73, 66.41, 54.25, 54.17, 53.20, 52.72, 28.81, 28.46, 23.47, 23.46; HRMS (ESI+) *m/z*: Calc. for $C_{31}H_{37}N_5O_4$: 544.2924 $[M+H]^+$. Found 544.2932 $[M+H]^+$.

4-Amino-8-(3-(piperidin-1-yl)propoxy)-2-(3-(3-(piperidin-1-yl)propoxy)phenyl)-5*H*-chromeno[4,3-d]pyrimidin-5-one (11c). Compound **5c** was treated with piperidine following the general procedure to give the desired product **11c** as a light brown solid with a yield of 30%. m.p. 118–120 °C; ^{1}H NMR (400 MHz, $CDCl_3$) δ 8.40 (d, J = 8.8 Hz, 1H), 8.20 (br d, J = 4.1 Hz, 1H), 8.11 (d, J = 7.8 Hz, 1H), 8.04 (s, 1H), 7.37 (t, J = 7.9 Hz, 1H), 7.06 (dd, J = 8.1, 2.5 Hz, 1H), 6.87 (dd, J = 8.8, 2.4 Hz, 1H), 6.70 (d, J = 2.3 Hz, 1H), 6.45 (br d, J = 4.0 Hz, 1H), 4.12 (t, J = 6.3 Hz, 2H), 4.04 (t, J = 6.3 Hz, 2H), 2.56 (t, 2H), 2.51 (t, 2H), 2.50–2.32 (m, J = 16.4 Hz, 8H), 2.10–1.97 (m, 4H), 1.69–1.57 (m, J = 10.5, 5.2 Hz, 8H), 1.52–1.39 (m, J = 4.6 Hz, 4H); ^{13}C NMR

(101 MHz, $CDCl_3$) δ 166.96, 163.53, 163.42, 162.04, 159.58, 159.10, 155.29, 138.54, 129.28, 126.69, 121.54, 118.23, 114.47, 113.09, 111.39, 101.10, 94.38, 66.91, 66.50, 56.02, 55.59, 54.60, 26.71, 26.43, 25.84, 25.77, 24.36, 24.32; HRMS (ESI+) *m/z*: Calc. for $C_{33}H_{41}N_5O_4$: 572.3237 $[M+H]^+$. Found 572.3249 $[M+H]^+$.

4-Amino-8-(3-(4-methylpiperazin-1-yl)propoxy)-2-(3-(3-(4-methylpiperazin-1-yl)propoxy)phenyl)-5*H*-chromeno[4,3-d]pyrimidin-5-one (11d). Compound **5c** was treated with *N*-methylpiperazine following the general procedure to give the desired product **11d** as a light brown solid with a yield of 31%. m.p. 115–117 °C; ^{1}H NMR (400 MHz, $CDCl_3$) δ 8.45 (d, J = 8.8 Hz, 1H), 8.23 (br d, J = 4.3 Hz, 1H), 8.12 (d, J = 7.8 Hz, 1H), 8.08–8.02 (m, J = 2.3, 1.5 Hz, 1H), 7.39 (t, J = 7.9 Hz, 1H), 7.06 (dd, J = 7.8, 2.2 Hz, 1H), 6.91 (dd, J = 8.8, 2.4 Hz, 1H), 6.75 (d, J = 2.3 Hz, 1H), 6.40 (br d, J = 4.3 Hz, 1H), 4.13 (t, J = 6.3 Hz, 2H), 4.07 (t, J = 6.3 Hz, 2H), 2.75–2.41 (m, 20H), 2.31 (s, 3H), 2.30 (s, 3H), 2.08–1.98 (m, 4H); ^{13}C NMR (101 MHz, $CDCl_3$) δ 167.08, 163.56, 163.47, 162.09, 159.69, 159.11, 155.36, 138.56, 129.33, 126.78, 121.56, 118.21, 114.56, 113.20, 111.47, 101.14, 94.45, 66.79, 66.33, 55.16, 54.99, 54.78, 53.08, 45.93, 26.76, 26.43; HRMS (ESI+) *m/z*: Calc. for $C_{33}H4_3N_7O_4$: 602.3455 $[M+H]^+$. Found 602.3472 $[M+H]^+$.

4-Amino-8-(3-(4-(2-hydroxyethyl)piperazin-1-yl)propoxy)-2-(3-(3-(4-(2-hydroxyethyl)piperazin-1-yl)propoxy)phenyl)-5*H*-chromeno[4,3-d]pyrimidin-5-one (11e). Compound **5c** was treated with *N*-(2-hydroxyethyl)piperazine following the general procedure to give the desired product **11e** as a light brown solid with a yield of 26%. m.p. 116–118 °C; ^{1}H NMR (400 MHz, $CDCl_3$) δ 8.34 (d, J = 8.8 Hz, 1H), 8.16 (br d, J = 3.8 Hz, 1H), 8.05 (d, J = 7.8 Hz, 1H), 7.98 (s, 1H), 7.33 (t, J = 7.9 Hz, 1H), 7.01 (dd, J = 8.1, 2.0 Hz, 1H), 6.82 (dd, J = 8.8, 2.3 Hz, 1H), 6.65 (d, J = 2.3 Hz, 1H), 6.57 (br d, J = 3.5 Hz, 1H), 4.07 (t, J = 6.1 Hz, 2H), 3.99 (t, J = 6.2 Hz, 2H), 3.66–3.56 (m, J = 5.5, 2.5 Hz, 4H), 3.15 (s, 2H), 2.65–2.36 (m, 24H), 2.03–1.92 (m, 4H); ^{13}C NMR (101 MHz, $CDCl_3$) δ 166.92, 163.46, 163.40, 161.98, 159.54, 159.05, 155.27, 138.53, 129.29, 126.69, 121.54, 118.09, 114.55, 113.09, 111.39, 101.05, 94.36, 66.68, 66.25, 59.47, 57.83, 55.18, 54.76, 53.19, 53.16, 52.86, 26.74, 26.37; HRMS (ESI+) *m/z*: Calc. for $C_{35}H_{47}N_7O_6$: 662.3666 $[M+H]^+$. Found 662.3670 $[M+H]^+$.

FRET assays

The labeled oligonucleotides F21T: 5-FAM-d(GGG[TTAGGG]$_3$)-TAMRA-3′ and F10T: 5′-FAM-dTATAGCTATA-HEG-TATAGCTATA-TAMRA-3′ were used as the FRET probes. Fluorescence melting curves were determined with a Roche LightCycler 2 real-time PCR machine, using a total reaction volume of 20 μL, with 0.2 μM of labeled oligonucleotide in 10 mM Tris-HCl buffer, pH 7.2, 60 mM KCl. Fluorescence readings with excitation at 470 nm and detection at 530 nm were taken at intervals of 1 °C over the range 37–99 °C, with a constant temperature being maintained for 30 s prior to each reading to ensure a stable value. The melting of the G-quadruplex was monitored alone or in the presence of various concentrations of compounds and/or of double-stranded competitor ds26 (5′-CAATCGGATCGAATTCGATCCGATTG-3′). Final analysis of the data was carried out using Origin 7.5 (OriginLab Corp.).

CD measurements

CD experiments were performed on a Chirascan circular dichroism spectrophotometer (Applied Photophysics). A quartz cuvette with 4 mm path length was used for the spectra recorded over a wavelength range of 230–450 at 1 nm bandwidth, 1 nm step size, and 0.5 s time per point. The oligomer HTG21 (5′-d(GGG[TTAGGG]$_3$)-3′) was diluted from stock to the required concentration (5 μM) in 10 mM Tris-HCl buffer, pH 7.2, 100 mM KCl, and then annealed by heating at 95 °C for 5 min, gradually cooled to room temperature, and incubated at 4 °C overnight. Then, CD titration was performed at a fixed HTG21 concentration (5 μM) with various concentrations (0–5 mol equiv) of the ligands in buffer containing 100 mM KCl at 25 °C. After each addition of ligand, the reaction was stirred and allowed to equilibrate for at least 10 min (until no elliptic changes were observed), and then a CD spectrum was collected. A buffer baseline was collected in the same cuvette, and subtracted from the sample spectra. Final analysis of the data was carried out using Origin 7.5 (OriginLab Corp.).

Surface plasmon resonance

SPR measurements were performed on a ProteOn XPR36 Protein Interaction Array system (Bio-Rad Laboratories, Hercules, CA) using a Neutravidin-coated GLH sensor chip. In a typical experiment, biotinylated HTG21 was folded in filtered and degassed running buffer (50 mM Tris-HCl, pH 7.2, 100 mM KCl). The DNA samples were then captured (~1000 RU) in flow cell 1, leaving the fourth flow cell as a blank. Ligand solutions (at 5, 2.5, 1.25, 0.625, 0.3125 μM) were prepared with running buffer by serial dilutions from stock solution. Five concentrations were injected simultaneously at a flow rate of 100 μL min^{-1} for 150 s of association phase, followed with 300 s of dissociation phase at 25 °C. The GLH sensor chip was regenerated with short injection of 50 mM NaOH between consecutive measurements. The final graphs were obtained by subtracting blank sensorgrams from quadruplex sensorgrams. Data are analyzed with ProteOn manager software, using the Equilibrium method for fitting kinetic data.

Molecular modeling

The crystal structure of the parallel 22-mer telomeric G-quadruplex (PDB ID 1KF1) was used as an initial model to study the interaction between the PBPP derivatives and telomeric DNA. For comparison with the DNA d(GGG[TTAGGG]$_3$) we used in the FRET and CD experiments, we removed the terminal 5′ adenine residue from the propeller-type structure and five adenines from each end of the hybrid-type structure to generate the 21-mer structure. Water molecules were removed from the PDB file, while the missing hydrogen atoms were added to the system using the Biopolymer module implemented in the SYBYL7.3.5 molecular modeling software from Tripos Inc. (St. Louis, MO). Ligand structures were constructed by adopting the empirical Gasteiger-Huckel (GH) partial atomic charges, and then were optimized (Tripos force field) with a nonbond cutoff of 12 Å and a convergence of 0.01 kcal mol^{-1}/Å over 10 000 steps using the Powell conjugate-gradient algorithm.

Docking studies were performed using the AUTODOCK 4.0 program.[50] By using ADT,[51] nonpolar hydrogens of the telomeric G-quadruplex were merged to their corresponding carbons, and partial atomic charges were assigned. The nonpolar hydrogens of the ligands were merged, and rotatable bonds were assigned. The resulting G-quadruplex structure was used as an input for the AUTOGRID program. AUTOGRID performed a precalculated atomic affinity grid maps for each atom type in the ligand plus an electrostatics map and a separate desolvation map present in the substrate molecule. The dimensions of the active site box, which was placed at the center of the G-quadruplex, were set to 60 Å × 60 Å × 60 Å with the grid point of 0.375 Å apart.

Molecular dynamics simulations were performed using the sander module of the AMBER 10.0 program suite. The nucleic acids were treated with the parm99 parameters.[52] The K^+ radius was kept at 2.025 Å.[53,54] Periodic boundary conditions were applied with the particle-mesh Ewald (PME) method[55] for long-range electrostatic interactions. The quadruplex and ligand complexes were solvated in a periodic TIP3P[56] water box with solvent layers of 10 Å. The potassium counterions were added to neutralize the complexes.

The hydrogen bonds were constrained using SHAKE.[57] For the nonbonded interactions, a residue-based cutoff of 10 Å was used. Temperature regulation was achieved by Langevin coupling with a collision frequency of 1.0. The solvated structures were subjected to initial minimization to equilibrate the solvent and counter cations. The G-quadruplex and inner K^+ ions were initially fixed with force constants of 100 kcal mol^{-1}. The system was then heated from 0 to 300 K in a 100 ps simulation, and followed with a 100 ps simulation to equilibrate the density of the system. Then, constant pressure MD simulation of 8 ns was performed in an NPT ensemble at 1 atm and 300 K. The output and trajectory files were saved every 10 ps for the subsequent analysis. All trajectory analysis was done with the Ptraj module in the Amber 10.0 suite, and examined visually using the VMD software package.[58]

The MM-PBSA method[59] implemented in the AMBER 10 suite was used to calculate the binding free energy between the G-quadruplex and the derivatives. All the waters and counterions were removed except the K^+ present within the negative charged central channel. The set of 500 snapshots from MD trajectories were collected to calculate the binding free energies.

TRAP-LIG assay

The activity of PBPP derivatives to inhibit telomerase in a cell-free system was assessed with the TRAP-LIG assay following previously published procedures.[44] Protein extracts from exponentially growing A549 leukemia cells were used. Briefly, 0.1 μg of TS forward primer (5′-AATCCGTCGAGCAGAGTT-3′) was elongated by telomerase (500 ng protein extract) in TRAP buffer (20 mM Tris-HCl, pH 8.3, 68 mM KCl, 1.5 mM $MgCl_2$, 1 mM EGTA, and 0.05% Tween 20) containing 125 μM dNTPs and 0.05 μg BSA. The mixture was added to tubes containing freshly prepared ligand at various concentrations and to a negative control containing no ligand. The initial elongation step was carried out for 20 min at 30 °C, followed with 94 °C for 5 min, and a final maintenance of the mixture at 20 °C. To purify the elongated product and to remove the bound ligands, the QIA quick nucleotide purification kit (Qiagen) was used according to the manufacturer's instructions. The purified extended samples were then subject to PCR amplification. In this step, a second PCR master mix was prepared consisting of 1 μM ACX reverse primer (5′-GCGCGG[CTTACC]$_3$CTAACC-3′), 0.1 μg TS forward primer (5′-AATCCGTCGAGCAGAGTT-3′), TRAP buffer, 5 μg BSA, 0.5 mM dNTPs, and 2 units of Taq polymerase. A 10 μL aliquot of the master mix was added to the purified telomerase-extended samples, and amplified for 35 cycles at 94 °C for 30 s, at 61 °C for 1 min, and at 72 °C for 1 min. Samples were separated on a 16% PAGE, and visualized with silver-staining. IC_{50} values were then calculated from the optical density quantitated from the AlphaEaseFC software.

Short-term cell viability

A549, HepG2, K562 and ECV-304 cells were seeded on 96-well plates (1.0×10^3 $well^{-1}$) and exposed to various concentrations of derivatives. After 48 h of treatment at 37 °C in a humidified atmosphere of 5% CO_2, 10 μL of 5 mg mL^{-1} methyl thiazolyl tetrazolium (MTT) solution was added to each well and further incubated for 4 h. The cells in each well were then treated with dimethyl sulfoxide (DMSO) (200 μL for each well), and the optical density (OD) was recorded at 570 nm. All drug doses were parallel tested in triplicate, and the IC_{50} values were derived from the mean OD values of the triplicate tests *versus* drug concentration curves.

Long-term cell culture experiments

Long-term proliferation experiments were carried out using the K562 leukemia cell line. Cells were grown in T80 tissue culture flasks at 1.0×10^5 per flask, and exposed to a subcytotoxic concentration of ligand or an equivalent volume of 0.1% DMSO every 4 days. The cells in control and drug-exposed flasks were counted and flasks reseeded with 1.0×10^5 cells. The remaining cells were collected and used for the measurements described below. This process was continued for 16 days.

SA-β-Gal assay

Cells treated with the ligand were incubated for 16 days. After the incubation, the growth medium was aspirated and the cells were fixed in 2% formaldehyde/0.2% glutaraldehyde for 15 min at room temperature. The fixing solution was removed, and the cells were gently washed twice with PBS, and then stained with the β-Gal staining solution containing 1 mg mL^{-1} of 5-bromo-4-chloro-3-indolyl-β-D-galactoside, followed with incubation overnight at 37 °C. The staining solution was removed, and the cells were washed three times with PBS. The cells were viewed under an optical microscope and photographed.

Telomere length assay

Cells treated with the ligand were incubated for 16 days. To measure the telomere length, genomic DNA was digested with Hinf1/Rsa1 restriction enzymes. The digested DNA fragments were separated on 0.8% agarose gel, transferred to a nylon membrane, and the transferred DNA was fixed on the wet blotting membrane by baking the membrane at 120 °C for 20 min. The membrane was hybridized with a DIG-labeled hybridization probe for telomeric repeats, and incubated with anti-DIG-alkaline

phosphatase. TRF was performed through chemiluminescence detection.

Acknowledgements

We thank the Natural Science Foundation of China (Grants U0832005, 90813011), the International S&T Cooperation Program of China (2010DFA34630), and the Science Foundation of Guangzhou (2009A1-E011-6) for financial support of this study.

References

1 J. T. Davis, *Angew. Chem., Int. Ed.*, 2004, **43**, 668–698.
2 S. Neidle and S. Balasubramanian, *Quadruplex Nucleic Acids*, RSC Publishing, Cambridge, 2006.
3 E. H. Blackburn, *Nature*, 1991, **350**, 569–573.
4 T. Simonsson, P. Pecinka and M. Kubista, *Nucleic Acids Res.*, 1998, **26**, 1167–1172.
5 D. Y. Sun, K. X. Guo, J. J. Rusche and L. H. Hurley, *Nucleic Acids Res.*, 2005, **33**, 6070–6080.
6 J. F. Riou, L. Guittat, P. Mailliet, A. Laoui, E. Renou, O. Petitgenet, F. Megnin-Chanet, C. Helene and J. L. Mergny, *Proc. Natl. Acad. Sci. U. S. A.*, 2002, **99**, 2672–2677.
7 A. Siddiqui-Jain, C. L. Grand, D. J. Bearss and L. H. Hurley, *Proc. Natl. Acad. Sci. U. S. A.*, 2002, **99**, 11593–11598.
8 T. M. Ou, Y. J. Lu, C. Zhang, Z. S. Huang, X. D. Wang, J. H. Tan, Y. Chen, D. L. Ma, K. Y. Wong, J. C. Tang, A. S. Chan and L. Q. Gu, *J. Med. Chem.*, 2007, **50**, 1465–1474.
9 D. Gomez, R. Paterski, T. Lemarteleur, K. Shin-Ya, J. L. Mergny and J. F. Riou, *J. Biol. Chem.*, 2004, **279**, 41487–41494.
10 A. M. Burger, F. P. Dai, C. M. Schultes, A. P. Reszka, M. J. Moore, J. A. Double and S. Neidle, *Cancer Res.*, 2005, **65**, 1489–1496.
11 A. De Cian, L. Lacroix, C. Douarre, N. Temime-Smaali, C. Trentesaux, J. F. Riou and J. L. Mergny, *Biochimie*, 2008, **90**, 131–155.
12 J. Seenisamy, E. M. Rezler, T. J. Powell, D. Tye, V. Gokhale, C. S. Joshi, A. Siddiqui-Jain and L. H. Hurley, *J. Am. Chem. Soc.*, 2004, **126**, 8702–8709.
13 X. D. Wang, T. M. Ou, Y. J. Lu, Z. Li, Z. Xu, C. Xi, J. H. Tan, S. L. Huang, L. K. An, D. Li, L. Q. Gu and Z. S. Huang, *J. Med. Chem.*, 2010, **53**, 4390–4398.
14 T. M. Ou, Y. J. Lu, J. H. Tan, Z. S. Huang, K. Y. Wong and L. Q. Gu, *ChemMedChem*, 2008, **3**, 690–713.
15 M. J. Moore, C. M. Schultes, J. Cuesta, F. Cuenca, M. Gunaratnam, F. A. Tanious, W. D. Wilson and S. Neidle, *J. Med. Chem.*, 2006, **49**, 582–599.
16 H. S. Huang, I. B. Chen, K. F. Huang, W. C. Lu, F. Y. Shieh, Y. Y. Huang, F. C. Huang and J. J. Lin, *Chem. Pharm. Bull.*, 2007, **55**, 284–292.
17 Y. J. Lu, T. M. Ou, J. H. Tan, J. Q. Hou, W. Y. Shao, D. Peng, N. Sun, X. D. Wang, W. B. Wu, X. Z. Bu, Z. S. Huang, D. L. Ma, K. Y. Wong and L. Q. Gu, *J. Med. Chem.*, 2008, **51**, 6381–6392.
18 H. Han, D. R. Langley, A. Rangan and L. H. Hurley, *J. Am. Chem. Soc.*, 2001, **123**, 8902–8913.
19 W. C. Drewe, R. Nanjunda, M. Gunaratnam, M. Beltran, G. N. Parkinson, A. P. Reszka, W. D. Wilson and S. Neidle, *J. Med. Chem.*, 2008, **51**, 7751–7767.
20 R. T. Wheelhouse, S. A. Jennings, V. A. Phillips, D. Pletsas, P. M. Murphy, N. C. Garbett, J. B. Chaires and T. C. Jenkins, *J. Med. Chem.*, 2006, **49**, 5187–5198.
21 K. M. Rahman, A. P. Reszka, M. Gunaratnam, S. M. Haider, P. W. Howard, K. R. Fox, S. Neidle and D. E. Thurston, *Chem. Commun.*, 2009, 4097–4099.
22 Z. A. Waller, P. S. Shirude, R. Rodriguez and S. Balasubramanian, *Chem. Commun.*, 2008, 1467–1469.
23 J. Dash, P. S. Shirude, S. T. Hsu and S. Balasubramanian, *J. Am. Chem. Soc.*, 2008, **130**, 15950–15956.
24 J. L. Zhou, Y. J. Lu, T. M. Ou, J. M. Zhou, Z. S. Huang, X. F. Zhu, C. J. Du, X. Z. Bu, L. Ma, L. Q. Gu, Y. M. Li and A. S. Chan, *J. Med. Chem.*, 2005, **48**, 7315–7321.
25 J. H. Tan, T. M. Ou, J. Q. Hou, Y. J. Lu, S. L. Huang, H. B. Luo, J. Y. Wu, Z. S. Huang, K. Y. Wong and L. Q. Gu, *J. Med. Chem.*, 2009, **52**, 2825–2835.
26 A. Sakurai, H. Midorikawa and Y. Hashimoto, *Bull. Chem. Soc. Jpn.*, 1971, **44**, 1677–1682.
27 M. M. Ismail and M. S. Mohamed, *Revue Roumaine de Chimie*, 1986, **31**, 533–539.
28 K. P. Ravindranathan, V. Mandiyan, A. R. Ekkati, J. H. Bae, J. Schlessinger and W. L. Jorgensen, *J. Med. Chem.*, 2010, **53**, 1662–1672.
29 B. Kuhn, P. Mohr and M. Stahl, *J. Med. Chem.*, 2010, **53**, 2601–2611.
30 R. J. Harrison, J. Cuesta, G. Chessari, M. A. Read, S. K. Basra, A. P. Reszka, J. Morrell, S. M. Gowan, C. M. Incles, F. A. Tanious, W. D. Wilson, L. R. Kelland and S. Neidle, *J. Med. Chem.*, 2003, **46**, 4463–4476.
31 D. Monchaud and M. P. Teulade-Fichou, *Org. Biomol. Chem.*, 2008, **6**, 627–636.
32 L. J. Farrugia, *J. Appl. Crystallogr.*, 1997, **30**, 565.
33 J. L. Mergny, L. Lacroix, M. P. Teulade-Fichou, C. Hounsou, L. Guittat, M. Hoarau, P. B. Arimondo, J. P. Vigneron, J. M. Lehn, J. F. Riou, T. Garestier and C. Helene, *Proc. Natl. Acad. Sci. U. S. A.*, 2001, **98**, 3062–3067.
34 A. De Cian, L. Guittat, M. Kaiser, B. Sacca, S. Amrane, A. Bourdoncle, P. Alberti, M. P. Teulade-Fichou, L. Lacroix and J. L. Mergny, *Methods*, 2007, **42**, 183–195.
35 P. A. Rachwal and K. R. Fox, *Methods*, 2007, **43**, 291–301.
36 A. D. Moorhouse, A. M. Santos, M. Gunaratnam, M. Moore, S. Neidle and J. E. Moses, *J. Am. Chem. Soc.*, 2006, **128**, 15972–15973.
37 A. De Cian, E. Delemos, J. L. Mergny, M. P. Teulade-Fichou and D. Monchaud, *J. Am. Chem. Soc.*, 2007, **129**, 1856–1857.
38 M.-P. Teulade-Fichou, C. Carrasco, L. Guittat, C. Bailly, P. Alberti, J.-L. Mergny, A. David, J.-M. Lehn and W. D. Wilson, *J. Am. Chem. Soc.*, 2003, **125**, 4732–4740.
39 E. M. Rezler, J. Seenisamy, S. Bashyam, M. Y. Kim, E. White, W. D. Wilson and L. H. Hurley, *J. Am. Chem. Soc.*, 2005, **127**, 9439–9447.
40 S. Paramasivan, I. Rujan and P. H. Bolton, *Methods*, 2007, **43**, 324–331.
41 P. Bates, J. L. Mergny and D. Yang, *EMBO Rep*, 2007, **8**, 1003–1010.
42 G. N. Parkinson, M. P. H. Lee and S. Neidle, *Nature*, 2002, **417**, 876–880.
43 W. L. DeLano, *The PyMOL Molecular Graphics System*, DeLano Scientific, San Carlos, CA, USA., 2002.
44 J. Reed, M. Gunaratnam, M. Beltran, A. P. Reszka, R. Vilar and S. Neidle, *Anal. Biochem.*, 2008, **380**, 99–105.
45 E. S. Hwang, *Mech. Ageing Dev.*, 2002, **123**, 1681–1694.
46 M. Sumi, T. Tauchi, G. Sashida, A. Nakajima, A. Gotoh, K. Shin-Ya, J. H. Ohyashiki and K. Ohyashiki, *Int. J. Oncol.*, 2004, **24**, 1481–1487.
47 T. Tauchi, K. Shin-ya, G. Sashida, M. Sumi, S. Okabe, J. H. Ohyashiki and K. Ohyashiki, *Oncogene*, 2006, **25**, 5719–5725.
48 J. M. Zhou, X. F. Zhu, Y. J. Lu, R. Deng, Z. S. Huang, Y. P. Mei, Y. Wang, W. L. Huang, Z. C. Liu, L. Q. Gu and Y. X. Zeng, *Oncogene*, 2006, **25**, 503–511.
49 F. C. Huang, C. C. Chang, P. J. Lou, I. C. Kuo, C. W. Chien, C. T. Chen, F. Y. Shieh, T. C. Chang and J. J. Lin, *Mol. Cancer Res.*, 2008, **6**, 955–964.
50 G. M. Morris, D. S. Goodsell, R. S. Halliday, R. Huey, W. E. Hart, R. K. Belew and A. J. Olson, *J. Comput. Chem.*, 1998, **19**, 1639–1662.
51 M. F. Sanner, *J. Mol. Graph. Model.*, 1999, **17**, 57–61.
52 W. D. Cornell, P. Cieplak, C. I. Bayly, I. R. Gould, J. Kenneth, M. Merz, D. M. Ferguson, D. C. Spellmeyer, T. Fox, J. W. Caldwell and P. A. Kollman, *J. Am. Chem. Soc.*, 1995, **117**, 5179–5197.
53 P. Hazel, J. Huppert, S. Balasubramanian and S. Neidle, *J. Am. Chem. Soc.*, 2004, **126**, 16405–16415.
54 P. Hazel, G. N. Parkinson and S. Neidle, *Nucleic Acids Res.*, 2006, **34**, 2117–2127.
55 T. Darden, D. York and L. Pedersen, *J. Chem. Phys.*, 1993, **98**, 10089–10092.
56 W. L. Jorgensen, J. Chandrasekhar, J. D. Madura, R. W. Impey and M. L. Klein, *J. Chem. Phys.*, 1983, **79**, 926–935.
57 J. P. Ryckaert, G. Ciccotti and H. J. C. Berendsen, *J. Comput. Phys.*, 1977, **23**, 327–341.
58 W. Humphrey, A. Dalke and K. Schulten, *J. Mol. Graph. Model.*, 1996, **14**, 33–38.
59 P. A. Kollman, I. Massova, C. Reyes, B. Kuhn, S. Huo, L. Chong, M. Lee, T. Lee, Y. Duan, W. Wang, O. Donini, P. Cieplak, J. Srinivasan, D. A. Case and T. E. Cheatham, 3rd, *Acc. Chem. Res.*, 2000, **33**, 889–897.

